Eur. Phys. J. B **11**, 505–512 (1999)

THE EUROPEAN PHYSICAL JOURNAL B

EDP Sciences

Self-assembled monolayers as interfaces for organic opto-electronic devices

L. Zuppiroli[1], L. Si-Ahmed[1], K. Kamaras[1,a], F. Nüesch[1,b], M.N. Bussac[2], D. Ades[3], A. Siove[3], E. Moons[4,c], and M. Grätzel[4]

[1] Laboratoire de Physique des Solides Semicristallins, Département de Physique, EPFL, 1015 Lausanne, Switzerland
[2] Centre de Physique Théorique, École Polytechnique, 91128 Palaiseau Cedex, France
[3] Institut Galilée, Université Paris-Nord, 93430 Villetaneuse, France
[4] Laboratoire de Photonique et Interfaces, Département de Chimie, EPFL, 1015 Lausanne, Switzerland

Received 3 December 1998 and Received in final form 6 April 1999

Abstract. Charge injection into an organic semiconductor can be improved by using a self-assembled monolayer of functionalized molecules grafted on the electrode. This new interface can be designed in order to reduce the Schottky barrier between the conductive electrode and the organic semiconductor. The polarizability of the molecules involved can also be chosen in order to increase the adhesion of the molecular semiconductor onto the electrode. We present Kelvin Probe experiments and saturated photovoltage measurements performed on a number of such derivatized electrodes. They permit a quantitative description of the potential shifts due to the self-assembled monolayers which are related to the electrical dipoles of the individual molecules constituting them. When conjugated sites contributing to the band states of the organic semiconductor are placed too close to the electrode in the negative part of the image-force potential, two new effects unfavorable to charge injection can appear. We demonstrate that it is convenient to separate the attachment group of the molecule from the conjugated core by a spacer of non-conjugated sites in order to reduce these undesirable effects.

PACS. 73.30.+y Surface double layers, Schottky barriers, and work functions – 73.61.Ph Polymers; organic compounds

1 Introduction

Monolayers of organic molecules, self-assembled on the surface of a semiconductor or a metal electrode can modify the electrochemical potential of the injected carriers. Such potential shifts are due to the permanent dipoles of the molecules organized at the electrode surface, the assembly of dipoles acting, far from the electrode, like an electrical double layer. The organic molecules used for this purpose have both functional groups for surface binding and auxiliary groups that participate to the molecule's dipole moment. Typical examples of such molecules used in the present work are given in Figures 1 and 2.

The potential energy shift $\Delta\chi$ due to the molecular monolayer can be expressed as $\Delta\chi = q\Gamma\mu/\varepsilon_0\varepsilon$ where $\Gamma = 10^{17}$ to $10^{18}/\mathrm{m}^2$ is the molecular surface concentration, $|\mu| = 1$ to 50 debye *i.e.* 3.3×10^{-30} to 1.7×10^{-28} Cm is the component of the dipole moment of the individual molecule perpendicular to the interface, $q = \pm 1.6 \times 10^{-19}$ C is the majority carrier charge, ε_0 the permittivity of the vacuum and ε the dielectric constant of the organic monolayer. This effect has already been directly witnessed on the surface of semiconductors either by using a Kelvin Probe or by photoemission spectroscopy [1–4]. The characteristics of organic diodes built with such derivatized electrodes have also been shown to depend in a crucial way on the electrical properties of such monolayers [5–11]. The potential shifts that can be obtained are substantial. A typical coverage of 10^{18} molecules/m^2 with small dipoles of 1 debye generates a potential energy shift of $\Delta\chi = 0.15$ eV. It was thus natural to try to control charge injection into organic electronic devices by using self-assembled monolayers.

Another reason to use these layers is to increase the adhesion of the organic film onto the metal or the oxide electrode. The quality of the interface, reflected by the degree of the structural order, has been improved substantially by using self-assembled monolayers (SAM) at the interfaces either in the organic transistor [12] or the organic light emitting diode [13]. This increase in electrode wettability

[a] Presently at Research Institute for Solid State Physics and Optics, Hungarian Academy of Sciences, P.O. Box 49, 1525 Budapest, Hungary
[b] Presently at Department of Chemistry, University of Rochester, Rochester, NY 14627-0216, USA
[c] Presently at Cavendish Laboratory, Madingley Road, Cambridge CB3 0HE, UK

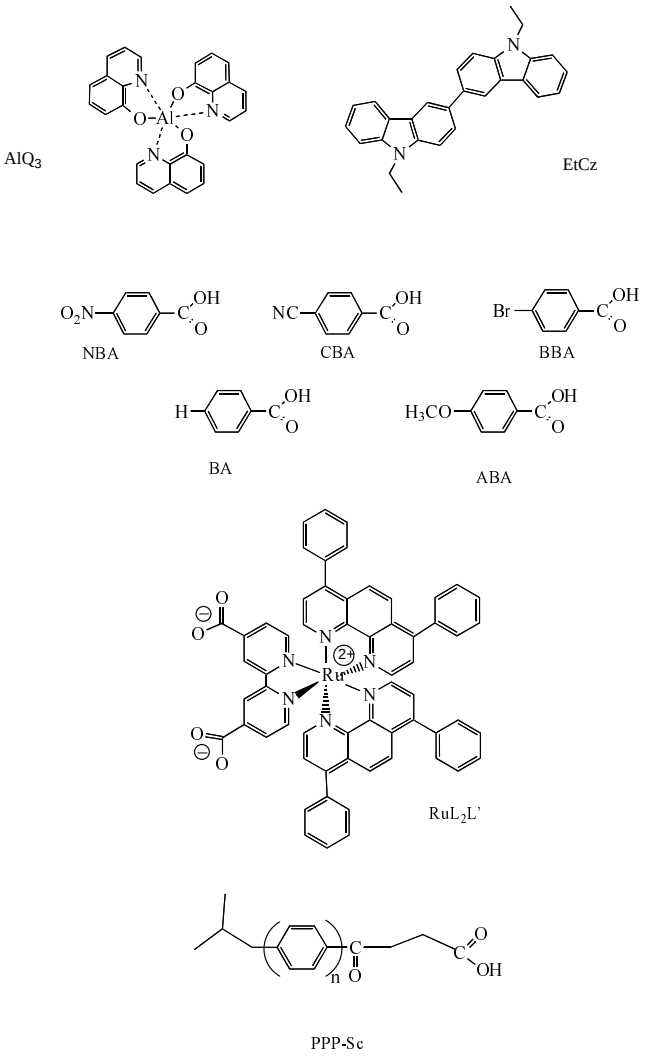

Fig. 1. Substances used to build self-assembled monolayers on indium tin oxyde electrodes (ITO). Commercially available products: *p*-nitrobenzoic acid (NBA), *p*-cyanobenzoic acid (CBA), *p*-bromobenzoic acid (BBA), *p*-benzoic acid (BA), *p*-anisobenzoic acid (ABA). Synthesized molecules: RuL_2L' complex (L = 4, 4′-diphenyl-1,10-phenantrolene, L′ = 4, 4′-dicarboxy-2,2′bipyridine); Poly-(paraphenylene) functionnalized with carboxylic acid (PPP-Sc). Electroluminescent molecules: aluminum tris-(8-hydroxyquinoline) (Alq_3) and bicarbazyl-N,N′-diethyl (EtCz).

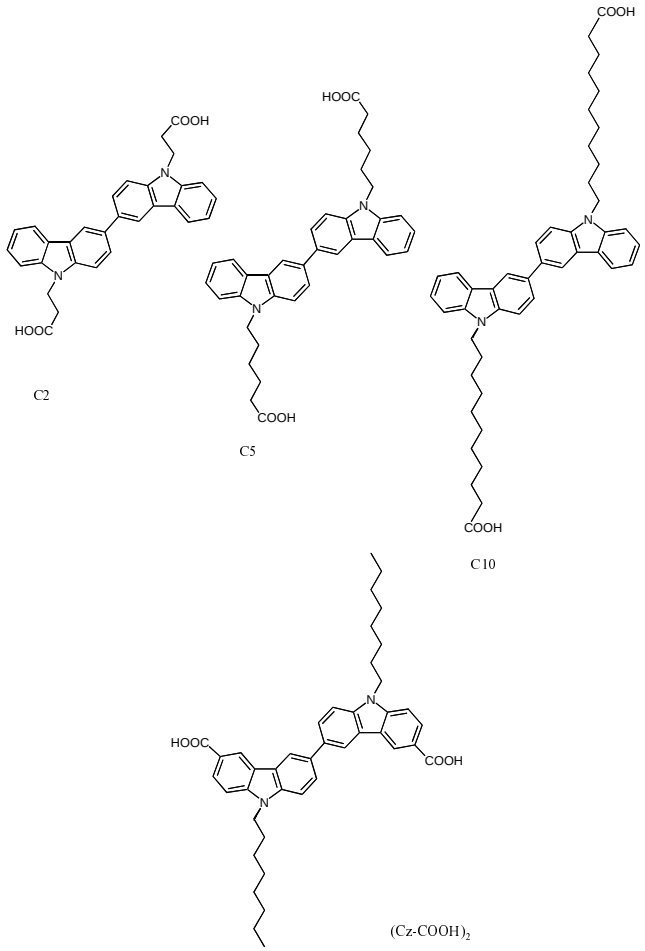

Fig. 2. Synthetized products used to build self-assembled monolayers on indium tin oxyde electrodes (ITO). Bicarbazyl-N,N′-dipropanoic acid (c2), bicarbazyl-N,N′-dihexanoic acid (c5), bicarbazyl-N,N′-di-undecanoic acid (c10), N,N′-dioctyl-3,3′-bicarbazyl-6,6′-dicarboxylic acid ($Cz\text{-}COOH)_2$.

with respect to the molecules of the organic semiconductor, can be attributed to the match between the molecular polarizability of the self-assembled monolayer to the polarizability of the organic material deposited onto it [13].

In the absence of a self-assembled monolayer, another effect, always negative in the sense that it is unfavorable for charge injection, can occur at the electrode/organic semiconductor interface of light emitting diodes. It is related to the presence of conjugated sites at a distance x_1 of the electrode with electron affinity χ_0 (respectively ionization potential π_0). In this case carriers can be transferred from the conductor to these sites and remain trapped in the negative part of the image force potential close to the metal interface [14]. The condition for this trapping to occur (in the case where electrons are the majority carriers) is $\chi_{(x_1)} < E_F$ where E_F is the bare metal Fermi energy and $\chi_{(x_1)} = \chi_0 - q^2/(16\pi\varepsilon_0\varepsilon x_1)$ is the electron affinity χ_0 corrected by the image force potential at the distance x_1. Here ε_0 is the permittivity of the vacuum and $\varepsilon \sim 3$ the dielectric constant of the organic semiconductor.

Far from the interface, these trapped charges can be viewed as a dipole layer formed at the metal-organic interface, *i.e.* a sort of planar condensator in which one plate of the electric double layer is the trapped charges at distance x_1 in the organic semiconductor while the other plate is the screening charge distribution placed at the surface of the metal. The closer the potentials E_F and χ_0 of the electrode and the semiconductor, the larger this unfavorable effect. For instance if 10^{18} sites/m^2 are available in the organic layer at a distance of 3.0 Å from the interface, and if the electron affinity of the organic sites $\chi_0 = -3.0$ eV is only 0.2 eV above the Fermi level of the electrode ($E_F = -3.2$ eV), then the double layer induced by trapping electrons at the interface, shifts

the potential energy far from the electrode by $\Delta\chi = 0.32$ eV. As a consequence, when the first layer is equilibrated with the electrode, the height of the Schottky barrier, which was initially 0.2 eV is now 0.52 eV.

Such an effect, predicted in reference [14] in the case where the organic semiconductor is a conjugated polymer, has been recently suspected in reference [15], where electron spectroscopy measurements (XPS and UPS) have been performed on calcium/phenylene-vinylene oligomer interfaces. During contact formation, a new peak appears in the UPS spectra of the junction which is attributed by the authors to "bipolaron states" filled in the first layers of the organic semiconductor. The same effect was also attributed a few years ago to bipolaron formation by Salaneck and Brédas [16]. But the best evidence of this image force effect, can be deduced from the recent work of Campbell and Smith [17] concerning electron injection into aluminum tris(-8-hydroxyquinolinate) (Alq_3). In this paper entitled "Schottky energy barriers and charge injection in metal/Alq/metal structures" they measure metal/Alq Schottky energy barriers for a range of contact metals with work functions from 2.7 eV (Sm) to 5.6 eV (Pt). They find that the electron Schottky barrier for metals with work functions higher than 4 eV ("bad" contacts) is basically the difference between the metal work function and the electron affinity of Alq_3 ($\sim$ 3 eV). But for metals of lower work functions, like calcium or samarium, for which no Schottky barrier would be expected because the Fermi level of the metal is situated above the LUMO of the organic semiconductor, they find that the electron Schottky barrier is actually pinned at about 0.6 eV. We interpret this important shift as being due to a monolayer of electrons trapped at a distance of about 5 Å of the interface on 10^{17} molecules/cm^2, in the negative part of the image force potential.

In the present paper we report both Kelvin Probe and saturated photovoltage measurements on a number of derivatized electrodes. The potential shifts measured directly and consistently on the self-assembled dipolar layers confirm the electrical behavior of the monolayers and permit the determination of molecular dipole in the presence of the electrode.

We have also specifically designed functionalized molecules with spacers of different lengths between the attachment group and the conjugated core (Fig. 2). Charge injection experiments performed on electrodes derivatized with the molecules of this series have confirmed the undesirable effect of the image force.

2 Experimental

2.1 Chemicals

All the molecules of the products used in the present work are presented in Figure 1. The attachment group of the functionalized molecules is always a carboxyl, intended to be fixed on the surface of oxides such as indium / tin oxide. Part of these materials are commercially available: aluminum tris(-8-hydroxyquinolate) (Alq_3), *p*-nitrobenzoic acid (NBA), *p*-cyanobenzoic acid (CBA), *p*-bromobenzoic acid (BBA), benzoic acid (BA), *p*-anisobenzoic acid (ABA) have been supplied by Aldrich (Fig. 1). Syntheses of some of the other products have already been described [6,14]: EtCz, RuL_2L', PPP-Sc, $(Cz\text{-}COOH)_2$. Three of them have been conceived and prepared for the present work: C2, C5, C10. Their carboxyl attachment group is separated from the polarizable core by a spacer of well defined length. Their syntheses are performed as follows: A mixture of carbazole (0.03 mole), the carboxylic spacer in its brominated form (example: 11-bromoundecanoic acid) (0.06 mole), sodium hydroxide (10 weight %), toluene and benzyltriethylammonium chloride is refluxed for 20 hours. After cooling, HCl (37%) is added till neutralization of the solution. The aqueous phase is removed from toluene (by phase separation) and the organic solution is washed with clean water. The carboxylic monomer is then esterified with methanol in the presence of a catalytic amount of sulfonic acid for 3 hours. After drying, the ester is dimerized with $FeCl_3$ in chloroform for 2 hours, followed by a hydrolysis catalyzed with sodium hydroxide and ended with acidification with sulfonic acid. The carboxylic acid dimer is then dried in vacuum (Fig. 2). All the materials were characterized by infrared spectroscopy, ^{1}H-NMR, ^{13}C-NMR and elemental analysis.

2.2 Coverage of the electrode by the self-assembled monolayer: Langmuir isotherms

The self-assembled monolayer is obtained by dipping the clean indium tin oxide electrode (from Balzers, 50 Ω/□) into a solution of the functionalized molecules. The cleaning procedure is standard [6] and ends in a glove box by a light argon plasma cleaning just before dipping the electrode into a solution of the functionalized molecules in tetrahydrofuran solvent. After several hours of grafting, the substrates were briefly rinsed in pure tetrahydrofurane, in order to remove the excess of unbounded molecules from the surface, and dried [9].

The potential energy shift across the self-assembled monolayer $\Delta\chi = q\Gamma\mu/\varepsilon_0\varepsilon$ depends on the surface concentration Γ of the molecules and their electrical dipole μ. It is thus essential to determine Γ, in each case, at the end of the grafting process. These data are obtained from the Langmuir isotherm measured by following carefully the procedure detailed in reference [18]. It consists basically in following the equilibrium between the adsorbate and the molecules in solution at different concentrations. The values of Γ obtained in such a way are listed in Table 1. They are all in the order of 10^{18} molecules/m^2. Figure 3 gives an example of the Langmuir isotherm for one of the molecules of interest in the present work.

2.3 Kelvin probe measurements

The contact potential difference method, or so called Kelvin probe technique, is a convenient method to measure the work function of a material. It can be used under

Table 1. We present the results of Kelvin Probe measurements (in air) and saturated photovoltage experiments performed on a number of self-assembled monolayers on ITO using the functionalized molecules represented in Figures 1 and 2. The density of molecules at the electrode has been measured by the Langmuir isotherm method and reported in the second column. The potential shifts ΔG and $\Delta G'$ measured by both techniques are comparable. Thus the molecular dipole can be finally determined ($\varepsilon = 5.3$ for molecules where the carboxylic acid is attached to the aromatic ring: $(\text{Cz-COOH})_2$, $\text{RuL}_2\text{L}'$, NBA, CBA, BBA, BA, ABA. and $\varepsilon = 2.5$ for esters: PPP-Sc, C2, C5, C10), ((a)=in air, (b)= in glove box).

		Kelvin probe measurements		Saturated photovoltage measurements			
Self-assembled monolayer	Surface concentration (molecules/m^2)	Work function G (eV)	ΔG (meV) $= G - G$ (ITO)	Counter electrode	Potential V_{bi}	$\Delta G'$ (meV) $= V_{\text{bi}} - (G_{\text{F}} - E_{\text{F}})$	Estimated dipole (debye)
PPP-Sc	2.4×10^{18}	−4.640	160	Al	0.7	200	0.4
$(\text{Cz-COOH})_2$	0.4×10^{18}	−4.66	140				4.9
C2	0.6×10^{18}	−4.6	200				2.2
C5	1.1×10^{18}	−4.55	250	Al	0.75	150	1.3
C10	0.8×10^{18}	−4.46	340				2.8
$\text{RuL}_2\text{L}'$	0.3×10^{18}	−4.280	520	Al	0.4	500	24
NBA	1.3×10^{18}	−4.980[a)]	−180	Al	0.75	150	−2
		−4.620[b)]	180				
CBA	3.0×10^{18}	−4.92	−120				−0.6
BBA	1.7×10^{18}	−4.86	−60				−0.5
BA	2.3×10^{18}	−4.38	420				2.5
ABA	2.0×10^{18}	−4.28	520				3.6
Reference				Al	0.9	0	
ITO		−4.8	0				
(plasma cleaned)				Mg/Ag	1.1	0	

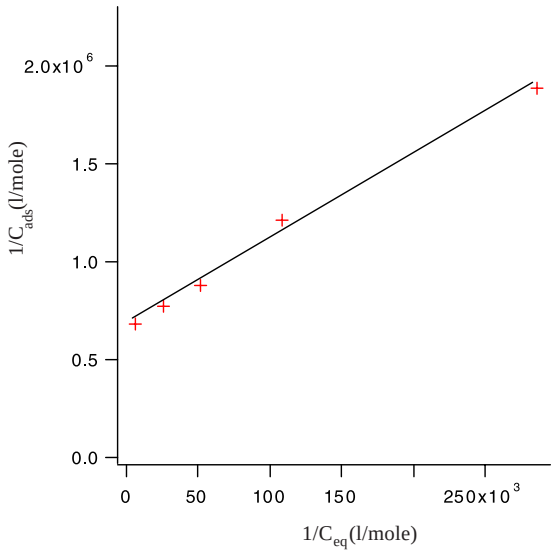

Fig. 3. Equilibrium between the solution and the adsorbate during the grafting process. A typical example of a Langmuir isotherm relates the inverse of the concentration of the adsorbate $1/C_{\text{ads}}$ on the electrode with the inverse of the concentration of the molecules in the solution $1/C_{\text{eq}}$. From the intercept of the curve, the molecular density on the electrode can be deduced [18]. The present example concern the $\text{RuL}_2\text{L}'$ complex ($T = 300$ K).

atmospheric conditions as well as in a glove box or in vacuum. From the difference between the value of the potential of a derivatized and a bare electrode, the potential shift due to the adsorbed self-assembled monolayer can be determined. The Kelvin probe is basically an electrostatic voltmeter which measures the contact potential difference between a given material and a material reference. The reference gold probe is placed as close as possible (< 1 mm) to the surface of interest. Both surfaces act as a capacitor which is charged when the work functions of the two materials are different. The charge is determined by vibrating the reference by means of a piezoelectric element, and is compensated by an external d.c. voltage. More details about the Kelvin probe can be obtained in reference [19]. The instrument that we used was manufactured by Delta Phi, Jülich, Germany.

The main cause of errors when this method is used to determine the potential difference across self-assembled monolayers is related to surface contaminants such as oxygen and water and to a slow evolution of the surface properties of ITO after plasma cleaning. An accurate comparison of experiments performed in air and in a glove box showed the error of the data of Table 1 to be ±0.1 eV.

2.4 Saturated photovoltage measurements

The saturated photovoltage measurements (SPM), makes use of two processes occurring in single-layer semiconductor devices. Illumination at higher frequencies than the gap of the semiconducting organic layer forms excitons. The presence of an electric field causes exciton dissociation producing a photocurrent. The electric field felt by the organic layer is the sum of the external potential

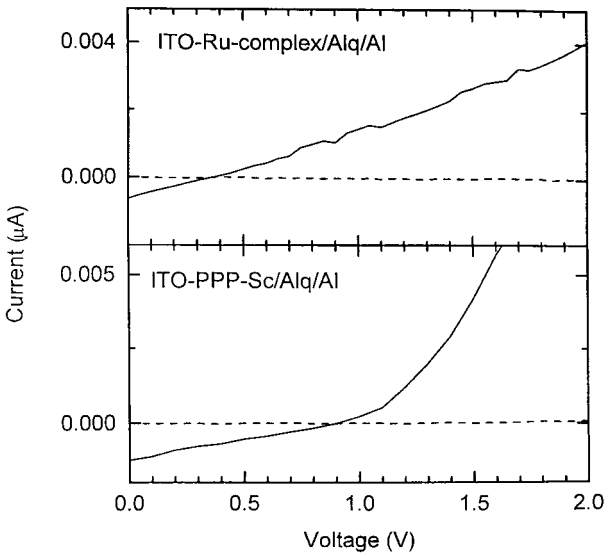

Fig. 4. Saturated photovoltage measurements. Current-voltage characteristics of single layer Alq_3 devices in the dark (dashed lines) and under saturated white light illumination at 16 mW/cm^2 (solid lines). The crossing yields the built-in potential V_{bi}. Both devices consist of 140 nm thick Alq_3 layers that are sandwiched between a chemically modified ITO anode and an aluminum cathode. The molecules used for the grafting on ITO are indicated in the graph.

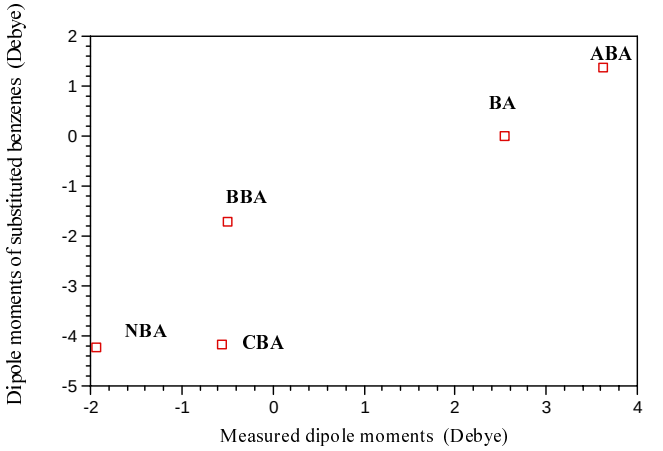

Fig. 5. Measured dipole moments of different benzoic acids attached on ITO electrodes *versus* the dipole moment of the corresponding substituted benzenes without carboxylic group, measured in the gas phase in reference [24].

and the built-in potential, V_{bi}, caused by the difference of workfunctions of the electrodes. If the applied potential balances the built-in field, the photocurrent is zero. Accordingly, the measurements consist of taking current-voltage characteristics at low field with and without illumination and determining the crossover of the dark and illuminated I-V curves [20,21]. The procedure has been applied to several known electrode combinations and the difference in electrode work functions was obtained with reasonable accuracy independent of the organic layer [22].

The method is not applicable to multilayer structures, where more sophisticated techniques (*e.g.* electroadsorption [23]) are necessary, but in case of derivatized ITO electrodes the change in work function could be followed reliably [7].

Saturation photovoltage measurements employed a tungsten halogen lamp for illumination at white incident light intensities between 16 mW/cm^2 and 17 mW/cm^2. The samples were kept in an argon dry box prior to the experiment. After mounting the contacts in air, they were transferred into a vacuum cryostat and measured at room temperature.

Figure 4 shows saturated photovoltage curves of two typical devices containing Alq_3 as organic layer in the presence of a self-assembled monolayer formed by a ruthenium complex (upper part) and a functionalized poly(paraphenylene) (lower part). The built-in potentials for all measured structures are summarized in Table 1. For all devices, the crossover of both curves with the dark current-voltage characteristics occurred at the same voltage, thus indicating saturation conditions where the crossover voltage becomes independent of the light intensity. In a few cases, notably with the carbazole-based devices we observed a rapid degradation under illumination. Therefore the values in Table 1 were recorded with fresh samples within a few minutes after loading them into the cryostat. Since degradation causes the measured V_{bi} to decrease, we took the maximum value as the lower limit for the true built-in potential.

3 Results and discussion

3.1 Kelvin probe and saturated photovoltage

The results of the Kelvin probe measurements on ITO derivatized electrodes are reported in Table 1. From the relation $\Delta\chi = q\Gamma\mu/\varepsilon_0\varepsilon$ presented in the introduction, the dipole moments μ of the molecules in presence of the ITO electrode were deduced. The numbers obtained vary from -2 debye to $+24$ debye. It is interesting to compare the adsorbed benzoic acids dipole moments with the literature data obtained with similar molecules without carboxylic acid groups measured in the vapour phase [24]. This comparison is made in Figure 5 which shows that the dipole moment of the carboxylates adsorbate is systematically shifted by $+2$ debye compared to the gaz phase values of the corresponding uncarboxylated molecules. Obviously this excess is due to the dipole moment of the extra carboxylic group in the presence of the ITO electrode. The dipole moment of the metanoic acid H-COOH in the gaz phase is 1.41 eV [24]. In the presence of the electrode, the possible protonation of the oxide surface by the carboxylic group is likely to enhance the total interfacial dipole moment [9] and reach this value of ≈ 2 debyes. Of course water adsorption or even solvant residues can modify this dipole moment substantially as shown in Table 1 for the case of the nitrobenzoic acid.

Our bare clean ITO electrodes exhibit a work function of -5.0 eV. After argon plasma the work function

increases by 0.2 eV. In the present work the Fermi level of our reference electrodes is then $G_F = -4.8 \pm 0.06$ eV with respect to vacuum. When an oxidative plasma is used the work function of ITO decreases to −5.4 eV.

The built in potential V_{bi} of the reference device ITO/Alq_3/Al corresponds to the difference between the Fermi levels $E_F = -4.0$ of aluminum and $G_F = -4.8$ eV of ITO, $V_{bi} = E_F - G_F \sim 0.8$ eV. In fact the experiment gives $V_{bi} = 0.9 \pm 0.1$. The replacement of aluminum by magnesium-silver electrode with a Fermi level at −3.7 eV gives $V_{bi} = E_F - G_F \sim 1.1$ eV which is confirmed experimentally. This result proves that there are no extrinsic electroactive traps acting in Alq_3 close to the electrode.

In both cases, our measurements are incompatible with the presence of charged layers close to the electrodes modifying the build-in potential of the device. This is simply due to the fact that the Fermi levels $E_F = -4.0$ eV (or −3.7 eV) and $G_F = -4.8$ eV of the electrodes are too different from the electron affinity $\chi_0 = -2.9$ eV and ionization potential $\pi_0 = -5.6$ eV of Alq_3. With the large Schottky barriers of 1.1 eV on the electron side and 0.8 eV on the hole side, the device is too blocking to permit any spontaneous flow of charges from the electrodes into the first layers of Alq_3, even in the presence of the image force. The condition of this flow to occur at the distance x_1 of the aluminum electrode would be:

$$E_F > \chi_{(x_1)} = \chi_0 - \frac{q^2}{16\pi\varepsilon\varepsilon_0 x_1}$$
$$\text{with } \chi_0 = -2.9 \text{ eV and } E_F = -4 \text{ eV}.$$

The result $x_1 < 0.9$ Å means that there are obviously no available sites of the Alq_3 molecule contributing to the LUMO state at such a distance from the electrode. This result is confirmed by the recent measurement of Campbell *et al.* who have shown that a simple Schottky model applies to aluminum electrodes [17].

On the side of the ITO electrode the condition for a charged layer to be formed at the distance y_1 of the hole injecting electrode is:

$$G_F < \pi_{(y_1)} = \pi_0 + \frac{q^2}{16\pi\varepsilon\varepsilon_0 y_1}$$
$$\text{with } G_F = -4.8 \text{ eV and } \pi_0 = -5.6 \text{ eV}.$$

The result, $y_1 < 1.3$ Å, implies that no significant charged layer can be formed on this side too. Thus in most experiments presented here, the organic semiconductor situated between the electrodes plays only a passive role in the saturated photovoltage measurements. The situation would have been different if a calcium electrode had been used instead of the aluminum one [17]. The most general device studied in the present work consists of a derivatized electrode, of an organic semiconductor like Alq_3 and of an aluminum counter electrode. The built in potential for such a blocking device just writes

$$V_{bi} = E_F - G_F + q\Gamma\mu/\varepsilon_0\varepsilon.$$

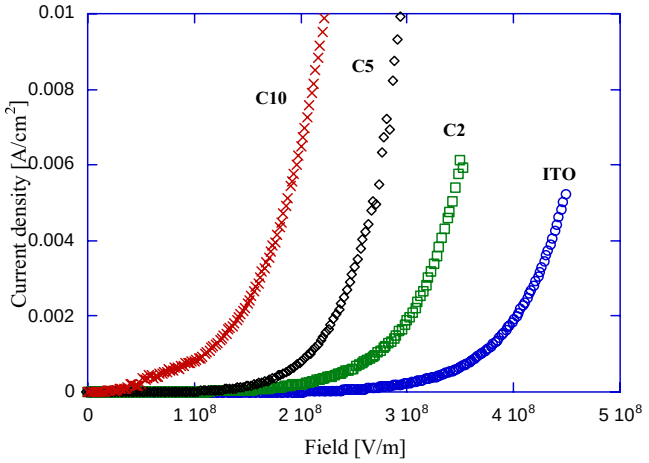

Fig. 6. Current *vs.* field characteristics of 4 hole only devices: derivatized ITO with C2/EtCz/Au (□), derivatized ITO with C5/ EtCz /Au (◊), derivatized ITO with C10/ EtCz /Au (×) and ITO/ EtCz /Au (○).

Table 1 demonstrates that, within our error limits, the Kelvin probe measurements and saturated photovoltage experiments give the same result.

3.2 Threshold voltages for injection from a derivatized electrode

In order to explore more accurately the effect of self-assembled monolayers on interfacial charge carrier transfer, functionalized molecules have been synthesized, endowed with an attachment group that is separated from the conjugated core by a saturated spacer of 2, 5 and 10 carbons respectively (Fig. 2). Monolayers from each of these 3 molecules were self-assembled onto ITO electrodes. These derivatized electrodes were used together with the diethyl-carbazole (Et-Cz) as organic semiconductor and a gold counter electrode.

Figure 6 shows the current-voltage characteristics of these single carrier devices where the current is carried by holes only. The injection thresholds are rather high because the barrier to injection is of the order of 1 eV. Surprisingly, the threshold decreases with increasing spacers length. Differences between the values of the dipole moments of the molecules cannot be invoked to understand this effect: Kelvin probe experiments performed on the three derivatized electrodes have measured the same dipole moment which shifts the Fermi level of ITO by about 200 meV. The dipole is oriented in such a way that it is unfavorable to hole injection. Moreover, in this kind of device, spontaneous charge transfer from the electrodes to the carbazole which would modify the Schottky barriers is highly improbable. As in the previous paragraph the Schottky barrier here is:

$$G_F - \pi_0 + \frac{q\Gamma\delta}{\varepsilon\varepsilon_0} \cong 1 \text{ eV}$$
$$(G_F = -4.8, \pi_0 = -5.6 \text{ eV and } q\Gamma\delta/\varepsilon_0 = 0.2 \text{ eV}).$$

Such a high barrier does not permit any significant charge transfer from the electrode to the organic semiconductor even in the presence of image force. The same is true on the gold side.

What is thus the reason of the positive effect on charge injection of an insulating spacer of about 1 nm placed at the electrode. Several authors have reported similar effects: just by evaporating a thin layer of 1 nm of insulating oxide, *i.e.* MgO or fluoride LiF at the interface with the cathode, two groups in Rochester [25] and in Tucson [26] have reported an important decrease of the injection threshold and an important increase of the electroluminescence efficiency of multilayer devices prepared with such an insulating layer. A group in Cambridge has recently controlled injection into polymer light emitting diodes by using ultrathin self-assembled layers of about 1 to 10 nm at the ITO interface [11]. If conducting polymer interlayers such as 5 nm auto doped polyaniline are well known to improve both carrier injection and electroluminescence efficiency, the positive effect of insulating polymer interlayers reported by this group [11] is probably of the same nature as the effect that we present here. Many interpretations have been proposed to explain this effect: tunneling injection [27], band bending [25], change of the work function of aluminum due to the presence of LiF [26], reduction of hole injection and confinement of the electrons to the emissive layer in order to reduce carrier leakage [11].

In our case we can exclude band bending because of the high injection barrier preventing any carrier flow, we can exclude work function changes because the work function has been measured and shown to be constant and we can exclude explanations related to current equilibration between electrons and holes because the current is carried by holes only. Additionally, we can exclude morphological effects since in all the three cases we are dealing with the same attachment groups and chromophores. Finally we emphazise that the presence of an 1 nm insulating barrier cannot suppress the charge transfer at the electrode, as the tunnel current through a 1 nm simple tunnel barrier of 5 eV height is still of the order of 1 A/cm^2, at least two orders of magnitude higher than usual currents crossing OLED's.

We believe that suppression of the image force experienced by the carriers at the interface is responsible for such an effect and will attempt to propose a general explanation of these effects in the next section.

3.3 The suppression of the undesirable effect of the image force by an insulating barrier

As in any metal/semiconductor interface the image force exerted on the charge carrier plays an important role at the interface between the electrode and the organic semiconductor [28,14]. This electrostatic effect results in a return of part of the carriers to the electrode. In other terms there is a zone close to the electrode where the electric field is opposite to the applied one. A crude estimation of the thickness x_n of this negative zone is obtained by searching the position of the maximum of the potential barrier

$$\chi_{(x)} = \chi_0 - qFx - \frac{q^2}{16\pi\varepsilon\varepsilon_0 x}$$

$$\text{which gives } x_n = \left(\frac{q}{16\pi\varepsilon\varepsilon_0 F}\right)^{1/2}.$$

For a field F of 1 MV/cm, one finds $x_n \sim 1$ nm. We think that the main effect of our non conjugated spacers or of an insulating barrier of lithium fluoride is just to avoid the coupling of the metal electrode with acceptor states situated in the attractive potential zone. The benefit that one can draw from the presence of this insulating layer which decouples the electrode from the π system of the organic semiconductor, depends on the value of the Schottky barrier $\chi_0 - E_F$ or $G_F - \pi_0$.

The experiments described here, deal with blocking contacts having Schottky barriers of the order 0.8 eV. In this case there is no significant charge trapping [17] and the effect of the insulating spacer is mainly to decrease the return current to the electrode. The less conjugated sites available in the negative part of the potential, the larger is the tunneling distance back to the electrode and the lower is the return current. Low return currents mean, for a given field, a larger net current injected into the device. When the barrier is lower, of the order of 0.2 eV or 0.3 eV as in the case of PPV on ITO cleaned by an oxygen plasma [29] the effect of an insulating spacer is different: as predicted in reference [14], when conjugated sites of the organic semiconductor are placed a few angstroms from a metal electrode, carriers flow from the metal to these sites and remain trapped in the image force potential. Since these trapped charges and their induced charge on the metal surface act as an electrical double layer the barrier $\chi_{(x)}$ is modified and becomes

$$\chi'_{(x)} = \chi_0 - qFx - \frac{q^2}{16\pi\varepsilon\varepsilon_0 x} + qS(x)$$

where $qS(x)$ is the generalized image force potential due to the trapped charges and defined in reference [14]. Given that this effect is due to the image force, it is always undesirable as it leads to an increase of the Schottky barrier with respect to a situation without the image force. In fact, for small bare Schottky barriers $|\chi_0 - E_F| < 0.5$ eV, the actual barrier is pinned at a value of the order of 0.5 eV as shown by Campbell and Smith in Alq_3 devices [17]. One way to avoid the unfavorable energy barrier is to eliminate the conjugated sites residing too close to the electrode by including a 1nm insulating spacer of any kind, which is not thick enough to suppress tunneling.

4 Conclusion

The quality of the interfaces of optoelectronic devices determines both the charge transfer from the metal contacts

and the durability and reliability of the device. The results presented in this paper show clearly that the use of monolayers, self-assembled at the interface, is indeed a good solution for improving this quality.

From this work we can deduce three criteria for an optimal design of the molecules constituting these self-assembled monolayers, in order to achieve better cohesion at the interface together with better charge transfer.

- It is convenient to provide the molecule with an electrical dipole typically from 5 to 15 debye in order to reduce the Schottky barrier and facilitate charge transfer. The dipolar moment of interest here is the total moment of the molecule including the attachment group in interaction with the substrate. We have shown in the case of the benzoic acids series, that this total dipole can be quite different than the dipole of the molecule alone in the gas phase.
- The self-assembled monolayer can also be designed in order to increase the adhesion between the organic semiconductor and the electrode. For this purpose, the polarizability of the molecules involved in the self-assembled monolayer should be matched to the polarizability of the organic semiconductor molecule [13].
- It is convenient to provide the molecule with a spacer of non-conjugated sites of about 1nm between the attachment group and the polarizable core of the molecule, in order to decouple the electrode and the organic semiconductor in a zone where the image force creates undesirable effects on injection.

We believe that self-assembled monolayers built with molecules fulfilling these three criteria will be very useful for building reliable organic optoelectronic devices.

We thank S. Goncalves-Conto for the help in the measurements of the current-voltage characteristics of Figure 6. This work was partially funded by the Swiss Science National Fundation under contract numbers 21-40435-94 and 20-52421.97 and by the optics priority program under contract number 121.

References

1. M. Bruening, E. Moons, D. Cahen, A. Shanzer, J. Phys. Chem. **99**, 8368 (1995).
2. J. Moser, P. Swarnalatha, P.P. Infelta, M. Grätzel, Langmuir **7**, 3012 (1991).
3. T.J. Meyer, G.J. Meyer, B.W. Pfenning, J.R. Schoonover, C.J. Timpson, J.F. Wall, C. Kobusch, X. Chen, B.M. Peek, C.G. Wall, W. Ou, B.W. Erickson, C.A. Bignozzi, Inorg. Chem. **33**, 3952 (1994).
4. A.J. Bard, L.R. Faulker, *Electrochemical Methods, Fundamentals and applications* (Wiley, New-York, 1980).
5. I.H. Campbell, S. Rubin, T.A. Zawodzinski, J.D. Kress, R.L. Martin, D.L. Smith, N.N. Barashkov, J.P. Ferraris, Phys. Rev. B **54**, R14321 (1996). .
6. F. Nüesch, L. Si-Ahmed, B. François, L. Zuppiroli, Adv. Mat. **9**, 222 (1997).
7. F. Nüesch, K. Kamaras, L. Zuppiroli, Chem. Phys. Lett. **283**, 194 (1998).
8. I.H. Campbell, J.D. Kress, R.L. Martin, D.L. Smith, Appl. Phys. Lett. **71**, 3528 (1997).
9. F. Nüesch, F. Rotzinger, L. Si-Ahmed, L. Zuppiroli, Chem. Phys. Lett. **288**, 861 (1998).
10. F.J. Appleyard, M.R. Willis, Opt. Mat. **9**, 120 (1998).
11. K.H. Ho, M. Granström, R.H. Friend, N.C. Greenham, Adv. Mat. **10**, 769 (1998).
12. H. Sirringhaus, N. Tessler, R. Friend, Science **280**, 1741 (1998).
13. S. Goncalves-Conto, M. Carrard, L. Si-Ahmed, L. Zuppiroli, Adv. Mat. **11**, 112 (1999).
14. M.N. Bussac, D. Michoud, L. Zuppiroli, Phys. Rev. Lett. **81**, 1678 (1998).
15. Y. Park, V.E. Choong, B.R. Hsieh, C.W. Tang, T. Wehrmeister, K. Müllen, Y. Gao, J. Vac. Sci. Technol. A **15**, 2574 (1997).
16. W.R. Salaneck, J.L. Brédas, Adv. Mat. **8**, 48 (1996).
17. L.H. Campbell, D.L. Smith, Appl. Phys. Lett. **74**, 561 (1999).
18. L. Si-Ahmed, F. Nüesch, B. François, L. Zuppiroli, Macromol. Chem. Phys. **199**, 625 (1998).
19. H. Lüth, *Surfaces and Interfaces of Solid Materials*, 3d edn (Springer), p. 464
20. X. Wei, M. Raikh, Z.V. Vardeny, Y. Yang, D. Moses, Phys. Rev. B **49**, 17480 (1994).
21. R.N. Marks, J.J.M. Halls, D.D.C. Bradley, R.H. Friends, A.B. Holmes, J. Phys.-Cond. Matter **6**, 1379 (1994).
22. X. Wei, S.A. Jeglinski, Z.V. Vardeny, Synth. Met. **85**, 1215 (1997).
23. I.H. Campbell, M.D. Joswick, I.D. Parker, Appl. Phys. Lett. **67**, 3171 (1995).
24. R.C. Weast, *CRC Handbook of Chemistry and Physics*, 57th edn, (CRC Press Cleaveland 1976), p. E-63-65.
25. L.S. Hung, C.W. Tang, M.G. Mason, Appl. Phys. Lett. **70**, 152 (1997).
26. S.E. Shaheen, G.E. Jabbour, M.M. Morrell, Y. Kawabe, B. Kippelen, N. Peyghambarian, J. Appl. Phys. **84**, 2324 (1998).
27. I.D. Parker, H.H. Kim, Appl. Phys. Lett. **64**, 1774 (1994).
28. Yu. N. Garstein, E. M. Conwell, Chem. Phys. Lett. **255**, 93 (1998).
29. C.C. Wu, C.I. Wu, J.C. Sturm, A. Khan, Appl. Phys. Lett. **70**, 1348 (1997).